

# An EEG Study on $\beta-\gamma$ Phase-Amplitude Coupling-Based Functional Brain Network in Epilepsy Patients

Junfeng Lu , Anyu Li , Kaijie Li , Renping Yu , Yuxia Hu , Rui Zhang , Lipeng Zhang , Hong Wan , and Mingming Chen 

**Abstract**—Epilepsy, a chronic neuropsychiatric brain disorder characterized with recurrent seizures, is closely associated with abnormal neural communications within the brain. Despite that the phase-amplitude coupling (PAC) has been suggested to offer a new way to observe neural interactions during epilepsy, however, few studies pay attention to alterations of the epileptic functional brain network based on PAC, especially on the  $\beta-\gamma$  PAC. Therefore, we use scalp electroencephalography (EEG) data of epileptic patients and the  $\beta-\gamma$  PAC modulation index (MI) to construct functional brain networks to examine variations of neural interactions during different epileptic phases. Statistically, the findings show that between-channel MI values in the post-ictal period significantly increase compared to that in the pre-ictal period, and the between-channel MI value has a close association with the information of phase and amplitude provided by the channels. Importantly, in both the phase-amplitude and amplitude-phase functional brain networks, the average node degree is remarkably higher in the post-ictal period than that in the pre-ictal period, whereas the characteristic path length in the ictal and post-ictal periods is significantly lower than that in the pre-ictal period. Besides, the average betweenness centrality in the post-ictal period is remarkably higher than that in the ictal period. Interestingly, the positive correlations between within-channel MI values and between-channel MI values can be observed during the pre-ictal, ictal and post-ictal periods. These findings suggest that the  $\beta-\gamma$  PAC-based functional brain network may provide a novel perspective

Manuscript received 17 July 2023; revised 15 December 2023 and 8 March 2024; accepted 14 March 2024. Date of publication 20 March 2024; date of current version 6 June 2024. This work was supported in part by the National Natural Science Foundation of China under Grant 62173310, in part by the MOST 2030 Brain Project under Grant 2022ZD0208500, and in part by the Technology Project of Henan Province under Grant 222102310031. (*Corresponding authors:* Hong Wan; Mingming Chen.)

Junfeng Lu, Anyu Li, Kaijie Li, Yuxia Hu, Lipeng Zhang, and Hong Wan are with the Henan Key Laboratory of Brain Science and Brain-Computer Interface Technology, School of Electrical and Information Engineering, Zhengzhou University, Zhengzhou 450001, China (e-mail: wanhang@zzu.edu.cn).

Renping Yu, Rui Zhang, and Mingming Chen are with the Henan Key Laboratory of Brain Science and Brain-Computer Interface Technology, School of Electrical and Information Engineering, Zhengzhou University, Zhengzhou 450001, China, and also with the Research Center for Intelligent Science and Engineering Technology of Traditional Chinese Medicine, School of Electrical and Information Engineering, Zhengzhou University, Zhengzhou 450001, China (e-mail: mmchen@zzu.edu.cn).

This article has supplementary downloadable material available at <https://doi.org/10.1109/JBHI.2024.3379194>, provided by the authors.

Digital Object Identifier 10.1109/JBHI.2024.3379194

to understanding alterations of neural interactions during the epileptic evolution, and may contribute to effectively controlling the spread of epileptic seizures.

**Index Terms**—Epilepsy, phase-amplitude coupling, modulation index, functional brain network.

## I. INTRODUCTION

EPILEPSY is a chronic neurological brain disease, and is closely related to abnormal neural oscillations observed on electroencephalography (EEG) [1]. Epileptic seizures are recurrent and uncertain, usually leading to damage to the central nervous system of patients and seriously affecting their physical and mental health [2]. Although the level of epilepsy treatment has greatly improved, about 30% of epilepsy patients worldwide still develop into intractable epilepsy due to insensitivity to antiepileptic drugs [3]. Moreover, the diversity of epileptogenic factors and the complexity of alternative neural interactions within the brain seriously hinder the effective treatment of intractable epilepsy [4]. Therefore, uncovering alterations of neural interactions during different epileptic phases may contribute to understanding transitions between non-ictal and ictal states, as well as mechanisms underlying the genesis of epilepsy.

Recently, growing evidence has suggested that epilepsy is a complex brain network disease, which is tightly associated with aberrant interactions between different brain regions [5], [6], [7]. Indeed, epileptic functional brain networks have been demonstrated to play crucial roles in localizing epileptogenic focus and understanding mechanisms of epilepsy transmission and controllability [8], [9], [10]. Of note, most of previous studies are often based on the phase information of epileptic EEG signals, using the phase locked value (PLV) and phase lag index (PLI) methods to construct epileptic functional brain networks [11], [12]. In contrast, due to the volume conduction and nonlinearity of EEG signals, few studies utilize the amplitude information-related correlation to construct functional brain networks [13]. However, it should be pointed out that both the phase and amplitude information of epileptic EEG signals have significant impacts on the construction of functional brain networks. Hence, to closely observe variations of functional brain networks, it is

necessary to combine the phase and amplitude information of epileptic EEG signals.

Phase-amplitude coupling (PAC) represents the coupling relationship between low-frequency phase and high-frequency amplitude of EEG signals [14]. In recent years, PAC has been commonly used to investigate neural interactions within the brain [15]. Especially, increasing evidence suggests that abnormal PAC may be associated with various neurological disorders, including Parkinson's disease, schizophrenia, Alzheimer's disease, and epilepsy [16]. For example, Ghinda et al. used intracranial EEG signals of ictal period to examine the dynamic evolution of modulation index (MI) PAC, and found that the locally increased PAC can be observed earlier than the onset of seizures [17]. Similarly, Hashimoto et al. found that the  $\theta$ - $\gamma$  PAC gradually increases along with the evolution of epilepsy and spreads from the local area to other brain regions [18]. Additionally, a recent animal experimental study has shown that the  $\theta$ - $\gamma$  PAC of epileptic rats in the interictal period is larger than that of normal rats, and deep brain stimulation could reduce the pathologically increased PAC, indicating that  $\theta$ - $\gamma$  PAC may contribute to predicting seizures and monitoring effectiveness of clinical treatment [19]. Obviously, PAC could provide a novel perspective to understanding neural interactions during different epileptic phases, as well as mechanisms underlying the onset and propagation of epileptic seizures.

However, it should be pointed out that the literature on neural interactions in epilepsy mainly focuses on the  $\theta$ - $\gamma$  PAC, whereas too little attention has been paid to the  $\beta$ - $\gamma$  PAC and the corresponding functional brain networks constructed with the  $\beta$ - $\gamma$  PAC. Rampp et al. calculated the coupling between the  $\gamma$  amplitude and  $\delta$ ,  $\theta$ ,  $\alpha$  and  $\beta$  phase of the iEEG data during the interval between attacks, and found that the PAC of each band in areas enriched for dysmorphic neurons increased, especially in the  $\delta$  or  $\theta$  bands [20]. Furthermore, certain studies on neurological disorders suggest that the PAC between  $\beta$  band and high-frequency band provides better explanatory power for signal variations than  $\beta$  band activity alone [21], [22]. Experimentally,  $\beta$  rhythm, which plays a role in various brain cognitive functions, has been confirmed as the most widespread cortical oscillatory activity during resting-state brain activity in epilepsy patients [23], [24], and the PAC between the low-frequency and gamma rhythms has been observed during epilepsy [18]. Accordingly, it is reasonable to speculate that alterations of the  $\beta$ - $\gamma$  PAC can be observed during different epileptic periods. If this hypothesis holds, it may complement the current commonly used  $\theta$ - $\gamma$  PAC methods for investigating neural interactions within the brains of epilepsy patients. To confirm this assumption, in the present study, we quantify  $\beta$ - $\gamma$  PAC by MI value calculated with EEG signals of intractable epilepsy patients, and construct the corresponding functional brain networks with MI values. Statistical analysis suggests that the  $\beta$ - $\gamma$  PAC of between-channels, as a whole shows an increasing trend during epileptic periods. Especially, the MI values of  $\beta$ - $\gamma$  PAC of between-channels in the post-ictal period are significantly higher than those during the pre-ictal period. Correspondingly, network analysis shows that both the average node degree and characteristic path length in the pre-ictal and

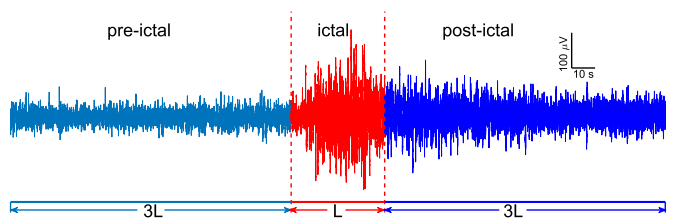


**Fig. 1.** An Example of EEG data segmentation.

post-ictal periods have significant differences. Of note, relative to the ictal period, the characteristic path length in the pre-ictal period increases remarkably, and the average betweenness centrality in the post-ictal period also increases remarkably. Moreover, the strong functional connectivity of F3-C3 brain region during different epileptic phases suggests that this brain region may play critical roles in the genesis of seizures. Interestingly, the average  $\beta$ - $\gamma$  PAC of within-channels is positively correlated with those of between-channels during epileptic periods. These results provide new ideas for understanding alterations of neural interactions within the brain during different epileptic phases, and may contribute to effectively controlling epileptic seizures.

## II. MATERIALS AND METHODS

### A. EEG Data and Preprocessing

The EEG data used in this work are acquired from the CHB-MIT Scalp EEG Database (<https://physionet.org/content/chbmit/1.0.0/>) jointly created by Children's Hospital Boston (CHB) and the Massachusetts Institute of Technology (MIT) [25]. These EEG data are recorded with the 10-20 international system, and the sampling rate is 256 Hz. Totally, 22 intractable epilepsy patients with 23 cases have been recorded, including 5 males aged 3-22 and 17 females aged 1.5-19.

Due to various differences of the EEG data for each epilepsy patient, the data selected to statistical analysis in the current study should satisfy a single seizure duration longer than 5 seconds. Notably, the priority has been considered to select the EEG data with an interval of more than 1 h between seizures. Accordingly, 6 hours EEG data of each epilepsy patient are selected, and there are 65 seizures in all selected data. Then, we use EEGLAB toolbox [26] to preprocess the selected raw EEG data. The average reference method is firstly used to re-reference the raw EEG data. To eliminate 60 Hz power frequency interference, the frequency component of 58-62 Hz in the data is filtered out through a notch filter. Lastly, independent component analysis (ICA) is employed to remove physiological artifacts in EEG signals.

Next, the preprocessed EEG data of each epilepsy patient is further selected based on the seizures marked by time labels. As shown in Fig. 1, assuming that the duration of the ictal period (red) is L seconds, in this work, we define the pre-ictal period (light blue) as 3 L seconds before the onset of seizure and the post-ictal period (blue) as 3 L seconds after the offset of seizure.

Note that the ictal data are divided into 5 seconds per segment, as well as the pre-ictal and post-ictal data. Accordingly, there are totally 195 data segments of the three periods, and each period has 65 data segments. Here, the  $\beta$  rhythm is in the frequency range from 13 to 30 Hz, and the  $\gamma$  rhythm is from 30 to 100 Hz. All data analysis and processing are performed on MATLAB 2021a.

### B. PAC Method

In the current study, we use the MI to quantify the  $\beta-\gamma$  PAC [27]. MI utilizes the Kullback-Leibler (KL) distance to measure the deviation of the high-frequency amplitude distribution-like function over low-frequency phase bins relative to the uniform distribution [15]. Specifically, the calculation of MI is as follows [27]:

- 1) Firstly, the original signal  $x_{raw}(t)$  is bandpass filtered to obtain low-frequency and high-frequency signals, and denoted as  $x_{f_P}(t)$  and  $x_{f_A}(t)$ , respectively.
- 2) Using the Hilbert transform to calculate the phase time series  $\Phi_{f_P}(t)$  of low-frequency signals  $x_{f_P}(t)$  and the amplitude time series  $A_{f_A}(t)$  of high-frequency signals  $x_{f_A}(t)$ , respectively.
- 3) Dividing the phase time series  $\Phi_{f_P}(t)$  into uniform intervals and calculating the corresponding means  $\langle A_{f_A} \rangle_{\Phi_{f_P}}$  of  $A_{f_A}(t)$  within each phase interval.
- 4) Normalizing the mean amplitude  $\langle A_{f_A} \rangle_{\Phi_{f_P}}$  as shown in (1).

$$P(j) = \frac{\langle A_{f_A} \rangle_{\Phi_{f_P}}(j)}{\sum_{k=1}^N \langle A_{f_A} \rangle_{\Phi_{f_P}}(k)}, \quad (1)$$

where  $\langle A_{f_A} \rangle_{\Phi_{f_P}}(j)$  is the average amplitude at the phase bin  $j$ , and  $N$  is the number of phase bins and typically set to  $N = 18$ .

- 5) Calculating KL distance. For the discrete distribution  $P$  and the discrete distribution  $Q$ , their KL distance is shown in (2).

$$D_{KL}(P, Q) = \sum_{j=1}^N P(j) \log \left[ \frac{P(j)}{Q(j)} \right], \quad (2)$$

where  $D_{KL}(P, Q) \geq 0$ .  $D_{KL}(P, Q) = 0$  if and only if  $P = Q$ , and at this point,  $P$  and  $Q$  represent the same distribution.

The Shannon entropy  $H(P)$  of the  $P$  distribution is defined as (3).

$$H(P) = - \sum_{j=1}^N P(j) \log[P(j)], \quad (3)$$

By combining (2) and (3), the relationship between KL distance and Shannon entropy can be obtained, as shown in (4).

$$D_{KL}(P, U) = \log(N) - H(P), \quad (4)$$

where  $U$  is a uniform distribution, and  $\log(N)$  is the potential maximum entropy value.

- 6) Finally, the Modulation index  $MI$  is defined, as shown in (5).

$$MI = \frac{D_{KL}(P, U)}{\log(N)}, \quad (5)$$

According to the definition of MI, it can be seen that  $0 \leq MI \leq 1$ . If and only if the high-frequency amplitude is uniformly distributed over the low-frequency phase, which is no phase-amplitude coupling and  $MI = 0$ . Clearly, the magnitude of the MI value is positively correlated with the deviation between the discrete distribution  $P$  and the uniform distribution  $U$ . It should be noted that the MI is calculated with phase in  $\beta$  frequency range and amplitude in  $\gamma$  frequency range, and the step size is 1 Hz.

### C. Topological Characteristics of $\beta-\gamma$ PAC-Based Functional Brain Networks

Traditional functional brain networks typically utilize the correlation or phase synchronization between signals to quantify the functional connectivity of different brain regions [28]. Numerous studies have shown that functional brain networks are able to effectively reveal interactions between different brain regions and contribute to deeply understanding epilepsy [10]. Given that MI calculated with the phase and amplitude information of EEG signals indirectly reflects neural interactions within the brain, which may be more suitable for constructing the functional brain network. Therefore, in this study, we use MI to construct the  $\beta-\gamma$  PAC-based functional brain network, and the specific process is as follows.

- 1) Based on (1) to (5), the MI value of  $\beta-\gamma$  PAC can be calculated by EEG signals of any two brain regions. For example, we denote the MI value between brain regions  $m$  and  $n$  as  $MI_{mn}$ , meaning that the  $MI_{mn}$  is calculated by EEG signals of brain regions  $m$  and  $n$ , which provide phase and amplitude information, respectively.

- 2) Constructing functional brain networks, and the corresponding MI-based connectivity matrix  $W_{MI}$  is defined in (6).

$$W_{MI} = \begin{pmatrix} MI_{m1} & MI_{m2} & \dots & 0 \\ \vdots & \vdots & \ddots & \vdots \\ MI_{21} & 0 & \dots & MI_{2n} \\ 0 & MI_{12} & \dots & MI_{1n} \end{pmatrix}, \quad (6)$$

To further reveal the topological characteristics of the functional brain networks at different epileptic phases, we analyze the node degree, the average node degree and the characteristic path length, which have been widely used to portray network characteristics in epilepsy research [29]. In this work, the node degree  $K_m$  of the  $m$ -th node in the functional brain network is calculated by (7).

$$K_m = \sum_{n=1}^N MI_{mn}, \quad (7)$$

where  $N$  is the number of network nodes, and  $MI_{mn}$  is the MI value of  $\beta-\gamma$  PAC between node  $m$  and node  $n$ .

Also, the calculation of the average node degree  $K$  of the functional brain network is shown in (8).

$$K = \frac{1}{N} \sum_{m=1}^N K_m, \quad (8)$$

The characteristic path length has been confirmed to be associated with the efficiency of brain information transmission, where the smaller the characteristic path length, the higher efficiency of brain information transmission and the stronger brain functional integration [30]. The characteristic path length of the functional brain network is calculated by (9).

$$L = \frac{1}{N(N-1)} \sum_{m,n \in V, m \neq n} l_{mn}, \quad (9)$$

where  $l_{mn}$  represents the shortest path length between the nodes  $m$  and  $n$ .

Betweenness centrality measures the number of shortest paths passing through a node, primarily to assess the node's ability to appear on the shortest paths between other nodes in the network, reflecting its importance in the process of network information transmission and its ability to serve as an information hub [31]. In the brain network, a higher value of average betweenness centrality indicates that nodes throughout the whole network are relatively important, which suggest that the information transmission in the network may be more uniform, rather than relying on a few nodes. On the other hand, a lower average betweenness centrality may indicate the presence of some important nodes in the network, while the betweenness centrality of other nodes is lower. Mathematically, the betweenness centrality of node  $m$  and the average betweenness centrality of the functional brain network are calculated by (10) and (11), respectively.

$$B_m = \frac{1}{(N-1)(N-1)} \sum_{m,n \in V, k \neq m, n \neq m, k \neq n} \frac{\rho_{kn}(m)}{\rho_{kn}}, \quad (10)$$

$$B = \frac{1}{N} \sum_{m=1}^N B_m, \quad (11)$$

where  $\rho_{kn}$  is the number of shortest paths between  $k$  and  $n$ , and  $\rho_{kn}(m)$  is the number of shortest paths between  $k$  and  $n$  that passes through  $m$ .

Of note, the minimum spanning trees (MSTs) and the eccentricity have also been applied in this study to overcome the potential biases caused by disconnected syndromes and to quantify the role of brain network node in information transmission, respectively [32], [33] (see the Supplementary Information).

#### D. Statistical Analysis

In the current study, two-sample t test is used to compare the differences in functional brain networks at different epileptic phases, and the test results are corrected by false discovery rate (FDR) at a level of 0.05. Moreover, because the data of network topological characteristics at different epileptic phases do not satisfy normal distribution, the rank sum test is used for statistical

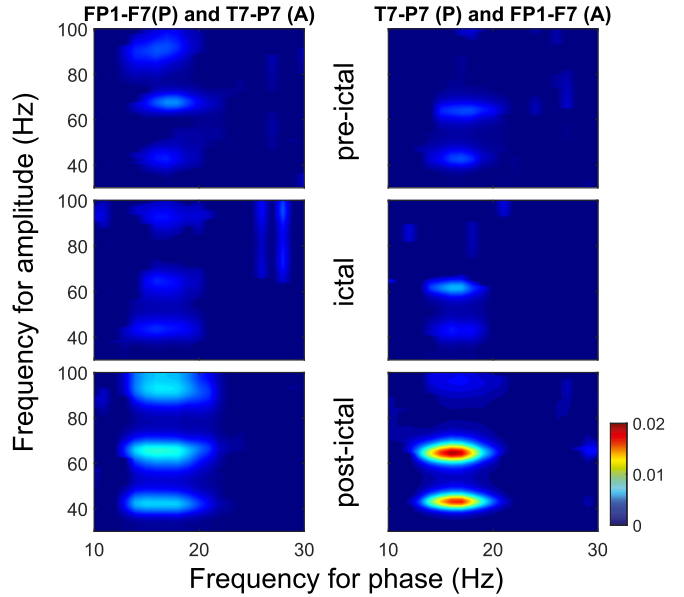


**Fig. 2.**  $\beta$ - $\gamma$  PAC between the FP1-F7 and T7-P7 channels of patient chb01.

comparisons. Also, the spearman rank correlation analysis is employed to investigate the relationship between the PAC coupling strength of within-channels and between-channels.  $P < 0.05$  indicates a statistically significant difference.

Additionally, it should be pointed out that to avoid pseudo MI values caused by data randomness, 200 random surrogate data have been used to calculate MI values, and the permutation test is conducted between the MI value calculated from the original data and that calculated from the surrogate data. The MI value is retained if  $P < 0.05$ , otherwise,  $MI = 0$ .

### III. RESULTS

#### A. $\beta$ - $\gamma$ PAC of Between-Channels At Different Epileptic Phases

Unlike the  $\theta$ - $\gamma$  PAC that has been widely used to investigate epilepsy, in the current study, we assume that the  $\beta$ - $\gamma$  PAC can also be observed during different epileptic phases, which may provide a new perspective to understanding neural interactions within the brain. To examine our assumption, three channel signals with electrode labeled FP1-F7, T7-P7, and P3-O1 are randomly selected to explore the potential  $\beta$ - $\gamma$  PAC of between-channels. Here, to distinguish the phase and amplitude information provided by different channels, we use "P" and "A" to denote the phase and amplitude information, respectively. For example, the labels FP1-F7(P), T7-P7(P) and P3-O1(P) represent the channels FP1-F7, T7-P7 and P3-O1 providing the phase information to calculate PAC. The labels FP1-F7(A), T7-P7(A) and P3-O1(A) denote the channels FP1-F7, T7-P7 and P3-O1 providing the amplitude information to calculate PAC.

Furthermore, we select the FP1-F7 and T7-P7 channels of patient chb01 to show that the  $\beta$ - $\gamma$  PAC can also be observed during different epileptic phases, as shown in Fig. 2. Obviously,

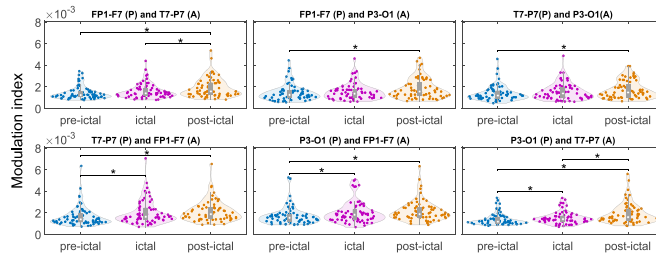


**Fig. 3.**  $\beta-\gamma$  PAC between FP1-F7, T7-P7, and P3-O1 channels of all patients.

as we expected, the  $\beta-\gamma$  PAC can be observed between the FP1-F7 and T7-P7 channels during the three epileptic periods. Intuitively, compared to the MI values of the pre-ictal and ictal periods, the MI values of  $\beta-\gamma$  PAC increase significantly in the post-ictal period. Interestingly, the increasing trend of MI values is not affected by the phase and amplitude information provided by the FP1-F7 and T7-P7 channels. However, the phase and amplitude information provided by each channel may have an influence on the strength of the  $\beta-\gamma$  PAC. Moreover, relative to the consistent distribution of the phase information, the distribution of central frequencies of the amplitude information is discrete. These results indicate that the  $\beta-\gamma$  PAC of between-channels may provide a new way to view the evolution of epilepsy, and the strength of  $\beta-\gamma$  PAC may be influenced by the type of information provided by the channels.

To quantify the alterations of  $\beta-\gamma$  PAC of between-channels at different epileptic phases, we use the rank sum test to analyze the statistical differences of MI values calculated with the FP1-F7, T7-P7 and P3-O1 channels during the three epileptic periods, as shown in Fig. 3. According to the statistical analysis, there are four types of alterations of MI values within the six cases combined by the three selected channels. Specifically, in terms of the first type combined by the FP1-F7(P) and T7-P7(A), the MI values in the post-ictal period are significantly higher than those in the ictal and pre-ictal periods. The combinations of the second type are involved in the FP1-F7(P) and P3-O1(A), T7-P7(P) and P3-O1(A), which show that the MI values in the post-ictal period are remarkably higher than those in the pre-ictal period. Unlike, in the third type combined by the T7-P7(P) and FP1-F7(A), P3-O1(P) and FP1-F7(A), the MI values in the ictal and post-ictal periods are significantly higher than those in the pre-ictal period. The combination of P3-O1(P) and T7-P7(A) is the fourth type, where the MI values in the post-ictal period are remarkably higher than those in the ictal and pre-ictal periods, and the MI values in the ictal period are also significantly higher than those in the pre-ictal period. Although the statistical differences of MI values are different in the four types, the MI values in the three epileptic periods, as a whole show an increasing trend. Particularly, the MI values of between-channels in the post-ictal period are significantly higher than those in the pre-ictal period.

Taken together, these results indicate that neural interactions alter with the evolution of epilepsy. Especially, the neural interactions within the brain may be at a relatively low level during

the pre-ictal period, whereas the level of neural interactions significantly increases after the offset of epileptic seizures.

### B. $\beta-\gamma$ PAC-Based Functional Brain Networks At Different Epileptic Phases

The above results show that the  $\beta-\gamma$  PAC of between-channels significantly alter with the epileptic phases, and the MI values are influenced by the phase and amplitude information provided by different channels. Theoretically, using the MI value of  $\beta-\gamma$  PAC to construct the functional brain network will greatly contribute to understanding neural interactions within the brain during different epileptic phases. Therefore, in the current study, it is very necessary to construct the  $\beta-\gamma$  PAC-based functional brain network. However, it should be pointed out that the MI values of  $\beta-\gamma$  PAC may be affected by the EEG signals recorded with close electrodes, which may lead to signal redundancy. Indeed, previous studies have demonstrated that the spatial position of the brain regions has remarkable impacts on the correlation of EEG signals [34]. To avoid these potential effects on MI values and also to reduce the computational cost, we randomly select eight channel signals with relatively dispersed recorded electrodes, which the corresponding labels are FP1-F7, T7-P7, P7-O1, FP1-F3, F3-C3, P3-O1, F8-T8 and FZ-CZ.

Based on the selected EEG signals, we use the MI values of  $\beta-\gamma$  PAC to construct the functional brain networks of different epileptic phases, as shown in Fig. 4. Note that the channels of the horizontal axis provide the amplitude information for calculating the MI, which the phase information is provided by the channels of the vertical axis. Besides the obvious alterations of the functional brain networks during the three epileptic periods, the functional brain networks are not symmetric, which is due to the asymmetry of phase and amplitude information provided by different channels (Fig. 4(a)). According to the asymmetric functional brain networks, we correspondingly construct two symmetric functional networks, which are the phase-amplitude network constructed with the functional connectivity of the triangle in the upper left (Fig. 4(b)) and the amplitude-phase network constructed with the functional connectivity of the triangle in the lower right (Fig. 4(c)). Despite the significant differences between the phase-amplitude and amplitude-phase networks during the three epileptic periods, the MI values gradually increase with the evolution of epilepsy in both brain networks. Moreover, we can observe that the FP1-F7 channel in the phase-amplitude network has higher MI values than that of other channels during the three epileptic periods. However, in the amplitude-phase networks, compared to other channels, both the FP1-F3 and F3-C3 channels have relatively higher MI values during the evolution of epilepsy.

To statistically quantify the alterations of  $\beta-\gamma$  PAC-based functional brain networks during the three epileptic periods, the paired two-sample t tests for the functional brain networks are conducted, and the false positive rate is controlled and corrected through the FDR to avoid spurious connections (edges), where the significant deviations between MI values are calculated, as

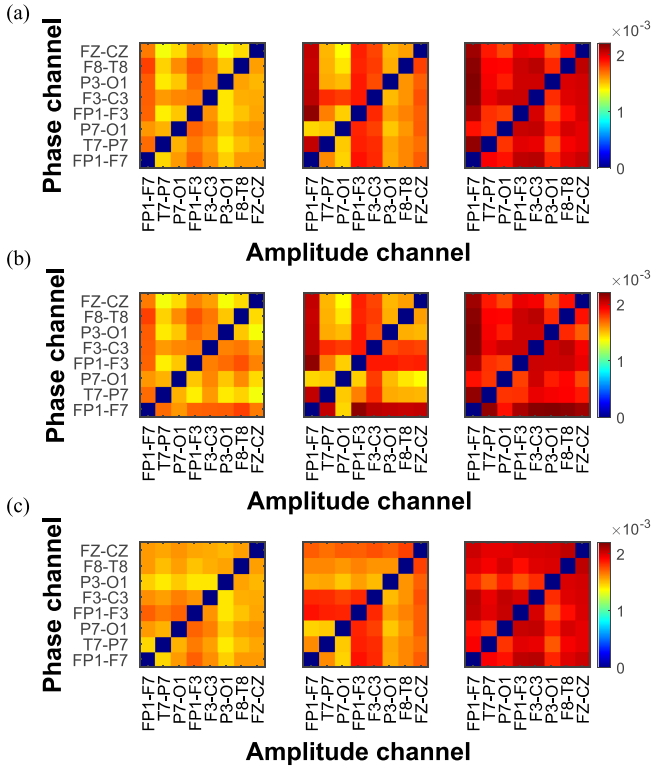


**Fig. 4.**  $\beta$ - $\gamma$  PAC-based functional brain networks in different epileptic phases. (a), Asymmetric functional brain network. (b), Phase-amplitude network; (c), Amplitude-phase network.

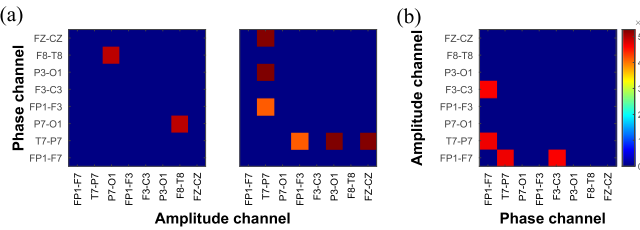


**Fig. 5.** Alterations of the  $\beta$ - $\gamma$  PAC-based functional brain networks during the evolution of epilepsy. (a), Significant changes in the phase-amplitude network. left: Compared to the ictal period, the enhanced MI values in the post-ictal period; right: compared to the pre-ictal period, the enhanced MI values in the post-ictal period. (b), Significant changes in the amplitude-phase network. Compared to the pre-ictal period, the enhanced MI values in the post-ictal period.

shown in Fig. 5. In terms of the phase-amplitude network, the MI value of  $\beta$ - $\gamma$  PAC between the F8-F8 and P7-O1 channels is significantly enhanced in the post-ictal period compared to that in the ictal period (Fig. 5(a)). Also, compared to the pre-ictal period, the MI values of  $\beta$ - $\gamma$  PAC between the T7-P7 and the other three channels, including the FP1-F3, P3-O1 and FZ-CZ channels, significantly enhanced in the post-ictal period (Fig. 5(a)). Interestingly, in the amplitude-phase networks, the MI values of  $\beta$ - $\gamma$  PAC between the FP1-F7 and other two channels that the F3-C3 and T7-P7 channels in the post-ictal period are significantly enhanced compared to that in the pre-ictal period (Fig. 5(b)). These results indicate that both the epileptic phases and information provided by EEG signals have important effects on the  $\beta$ - $\gamma$  PAC-based functional brain networks.

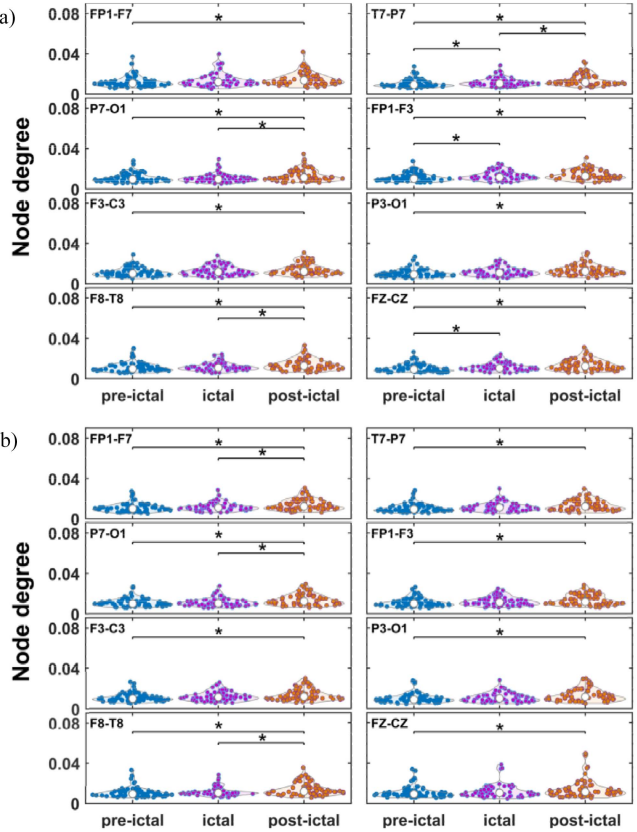


**Fig. 6.** The Node degree of the  $\beta$ - $\gamma$  PAC-based functional brain network during different epileptic phases. (a), the node degree of the phase-amplitude network. (b), the node degree of the amplitude-phase network.

### C. Topological Characteristics of $\beta$ - $\gamma$ PAC-Based Functional Brain Networks During Epileptic Phases

To further investigate alterations of topological characteristics of  $\beta$ - $\gamma$  PAC-based functional brain networks during the three epileptic periods, we firstly calculate the degree of each node in the phase-amplitude and amplitude-phase networks, respectively (Fig. 6). Note that the functional brain network has 8 nodes and 65 seizures. Intuitively, the statistical differences of node degree are obvious during different epileptic phases. The common change observed in the two networks is that all node degrees exhibit a significant increase in the post-ictal period compared to that in the pre-ictal period. Besides, in the phase-amplitude network, the node degree of the T7-P7, P7-O1 and F8-T8 channels in the post-ictal period also significantly increases compared to that in the ictal period, but compared to that observed in the pre-ictal period, the node degree of the T7-P7, FP1-F3 and FZ-CZ channels increases significantly in the ictal period (Fig. 6(a)). Of note, the remarkable differences of the node degree during the three epileptic periods can only be observed in the T7-P7 channel. Similarly, in the amplitude-phase network, compared to the node degree observed in the ictal period, the node degree of the FP1-F7, P7-O1 and F8-T8 channels also shows significant increase in the post-ictal period (Fig. 6(b)).

**TABLE I**  
CHANNEL CLASSIFICATION BASED ON THE NODE DEGREE OF PHASE-AMPLITUDE NETWORK

Classification Number	Channel	Statistical differences
1	FP1-F7/F3-C3 /P3-O1	Compared to the pre-ictal period, the node degree significantly increases in the post-ictal period.
2	P7-O1/F8-T8	Compared to the pre-ictal and ictal periods, the node degree significantly increases in the post-ictal period.
3	FP1-F3/FZ-CZ	Compared to the pre-ictal period, the node degree significantly increases in the ictal and post-ictal periods.
4	T7-P7	Compared to the pre-ictal and ictal periods, the node degree significantly increases in the post-ictal period, and compared to the pre-ictal period, the node degree significantly increases in the ictal period.

**TABLE II**  
CHANNEL CLASSIFICATION BASED ON THE NODE DEGREE OF AMPLITUDE-PHASE NETWORK

Classification Number	Channel	Statistical differences
1	T7-P7/FP1-F3 /F3-C3/P3-O1 /FZ-CZ	Compared to the pre-ictal period, the node degree significantly increases in the post-ictal period.
2	FP1-F7/P7-O1 /F8-T8	Compared to the pre-ictal period, the node degree significantly increases in the ictal and post-ictal periods.

Together, despite that the increased trend of the node degree is the same in the post-ictal period, alterations of the node degree of the two  $\beta$ - $\gamma$  PAC-based functional brain networks during the three epileptic periods are partially different, which may be associated with the phase or amplitude information provided by each channel. Furthermore, to observe the consistent alterations of the node degree during different epileptic phases, the EEG channels are divided into four categories in the phase-amplitude network (Table I), as well as two categories in the amplitude-phase network (Table II). Interestingly, although the number of category is different for the two functional brain networks, the statistical differences of several EEG channels are the same, such as P7-O1, F3-C3, P3-O1 and F8-T8 channels. Theoretically, the various changes of the node degree indicate that these nodes may have different contributions to the dynamical evolution of epilepsy, which may also provide a new way to localize the epileptic zone.

Additionally, to observe alterations of the global network property during epileptic phases, the average node degree of the two functional brain networks is calculated (Fig. 7). Obviously, the average node degree of the two functional brain networks in the post-ictal period is significantly higher than that in the pre-ictal period, which is consistent with the findings observed in the node degree of each channel (see Fig. 6). These observations indicate that the sparsity of functional brain networks may be lower in the post-ictal period, meaning that the neural

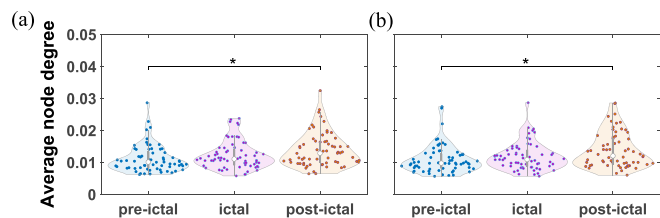


**Fig. 7.** The Average node degree of the  $\beta$ - $\gamma$  PAC-based functional brain networks during epileptic phases. (a), the average node degree of the phase-amplitude network. (b), the average node degree of the amplitude-phase network.

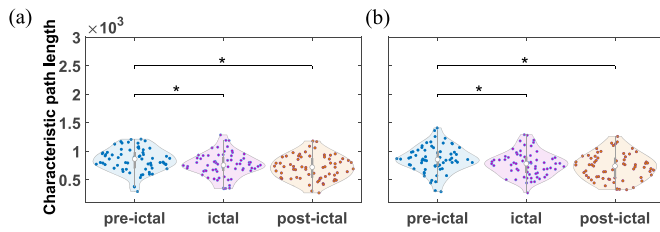


**Fig. 8.** Characteristic path length of the  $\beta$ - $\gamma$  PAC-based functional brain networks during epileptic phases. (a), the characteristic path length of the phase-amplitude network. (b), the characteristic path length of the amplitude-phase network.

interactions within the brain may be enhanced in the post-ictal period.

Also, to observe changes of the information transmission efficiency within the two functional brain networks during epileptic phases, we calculate the characteristic path length of these networks (Fig. 8). Statistically, the characteristic path length of the two functional brain networks in the ictal and post-ictal periods is significantly reduced compared to that in the pre-ictal period. However, there is no significant difference between the ictal and post-ictal periods. These results indicate that epileptic seizures may have remarkable effects on the information transmission efficiency, which may strengthen the functional integration ability of the brain.

Accordingly, it is reasonable for us to speculate that the significant changes of the characteristic path during epileptic phases may provide a potential biomarker for predicting seizures.

Similarly, to analyze the changes of information transmission uniformity within the two functional brain networks during epileptic phases, we calculate the average betweenness centrality of these networks (Fig. 9). Statistically, the average betweenness centrality of the two functional brain networks in the post-ictal period significantly increases compared to that in the ictal period. These results suggest that during seizures, several key nodes may play a dominant role in information transmission in the brain network. However, in the post-ictal period, information transmission in the brain network no longer relies on a few key nodes and becomes more evenly distributed. Of note, the betweenness centrality of each node in both the phase-amplitude and amplitude-phase networks has also been calculated and statistically analyzed (see Fig. S1 in the Supplementary Information). The statistical results indicate that the betweenness

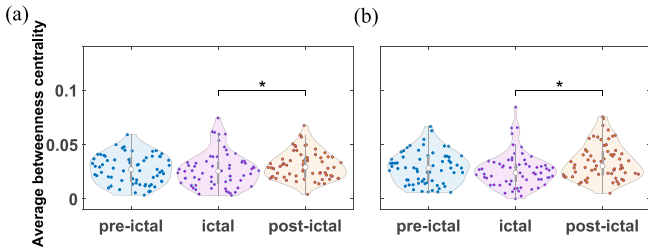


**Fig. 9.** The Average betweenness centrality of the  $\beta$ - $\gamma$  PAC-based functional brain networks during epileptic phases. (a), the average betweenness centrality of the phase-amplitude network. (b), the average betweenness centrality of the amplitude-phase network.

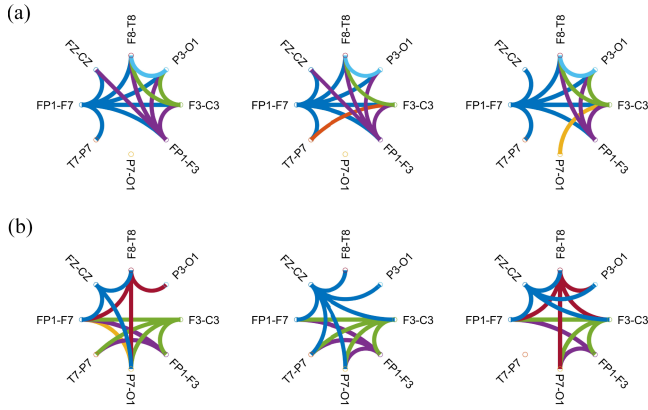


**Fig. 10.** The Functional brain network connectivity of  $\beta$ - $\gamma$  PAC during epileptic phases. (a), phase-amplitude network. (b), amplitude-phase network.

centrality of each node in the two functional brain networks changes variously during different epileptic phases. Interestingly, the betweenness centrality of each node observed in the ictal period often shows significantly decrease compared to that in the pre-ictal and post-ictal periods, which is partly consistent with observations in Fig. 9.

Along with the changes of network property observed in the two  $\beta$ - $\gamma$  PAC-based functional brain networks, theoretically, the alterations of functional connectivity of the two networks should be remarkable. As shown in Fig. 10, the functional connectivities of the top 20% of each network have been selected to show the variations during epileptic phases. It is easy to observe that besides the significant changes of functional connectivity in the phase-amplitude and amplitude-phase networks, the variations of functional connectivity are different for the two networks.

Obviously, there are differences in phase-amplitude network connectivity during different epileptic phases, as shown in Fig. 10(a). Specifically, the functional connectivity of the phase-amplitude network mainly exists in the FP1-F7, FP1-F3 and F3-C3 brain regions, among which the functional connectivity between the FP1-F7 and other brain regions remains stable during different epileptic phases. Similarly, the connectivity of the amplitude-phase network during different epileptic phases is also different, as shown in Fig. 10(b). However, compared with phase-amplitude network, amplitude-phase network connectivity varies more during different epileptic phases. Specifically, functional connectivity of the amplitude-phase network mainly

exists in the FZ-CZ and F3-C3 brain regions, suggesting that the overall information interaction between the FZ-CZ and F3-C3 brain regions may be stronger during different epileptic phases. Notably, in the ictal period, connection between FZ-CZ and other brain regions is enhanced and that between F8-T8 and other brain regions is weakened, suggesting that seizures may enhance information interaction between FZ-CZ and other brain regions, but may inhibit information interaction between F8-T8 and other brain regions. These results indicate that the functional connectivity of the two functional brain networks varies during different epileptic phases, and that of the amplitude-phase network varies comparatively more. The F3-C3 region showed strong functional connectivity in two functional brain networks, indicating that the F3-C3 region may be a key brain region in seizures.

In addition, to overcome the potential biases caused by disconnected syndromes, the minimum spanning trees (MSTs) of the phase-amplitude and amplitude-phase networks have been computed (see Fig. S2 in the Supplementary Information). Obviously, the FP1-F7 region has more connections than other brain regions during different epileptic phases, which is consistent with observations in Fig. 10. Furthermore, the average eccentricity of the two functional brain networks based on the MSTs has also been calculated (see Fig. S3 in the Supplementary Information). Although no significant difference of the average eccentricity can be observed in each functional brain network, the significant changes of the eccentricity of several brain regions still can be observed during epileptic phases (see Fig. S4 in the Supplementary Information), which further support the observations in Fig. 10.

#### D. The Relationship of $\beta$ - $\gamma$ PAC Between Within-Channels and Between-Channels During Epileptic Phases

As mentioned above, the  $\beta$ - $\gamma$  PAC-based functional brain networks significantly change with the evolution of epilepsy. However, it should be pointed out that both the phase-amplitude and amplitude-phase networks are constructed by different EEG channels, which the information of phase and amplitude is provided by two different channels. Correspondingly, a question that whether there exists a relationship of  $\beta$ - $\gamma$  PAC between within-channels and between-channels during epileptic phases may be arisen. To examine this question, we use the Spearman rank correlation to analyze the potential relationship. Of note, the within-channel MI value is calculated with phase and amplitude provided by the same channel, and then averaging these MI values to obtain the averaged within-channel MI value. Correspondingly, the between-channel MI value is calculated with phase or amplitude from one channel but amplitude or phase provided by all other channels, and then calculating the mean of these MI values to obtain the averaged between-channel MI value.

As shown in Fig. 11, the positive correlations of averaged  $\beta$ - $\gamma$  PAC between within-channels and between-channels are significant and different during the three epileptic periods. Importantly, the information of phase and amplitude has different influences

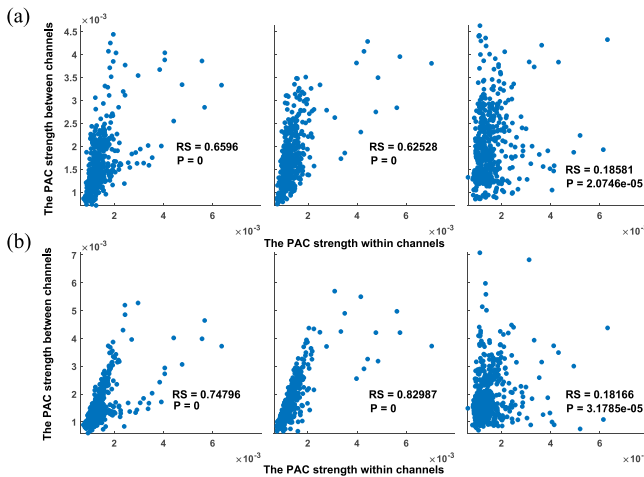


**Fig. 11.** Relationship of  $\beta$ - $\gamma$  PAC between within-channels and between-channels during epileptic phases. (a), the between-channel MI value calculated with one channel providing phase information. (b), the between-channel MI value calculated with one channel providing amplitude information. RS represents the correlation coefficient and P represents the significance level. P=0 indicates that P approaches 0.

on the between-channel MI values, which the correlation coefficients are higher for the case that one channel provides amplitude information and all other channels provide phase information during the pre-ictal and ictal periods (Fig. 11(b)). However, in the post-ictal period, both the phase and amplitude information may have less effects on the correlation coefficients, which are relatively smaller than that in the pre-ictal and ictal periods. These observations suggest that the neural interactions may be more complex during the post-ictal period.

#### IV. DISCUSSION

The PAC has been suggested to play key roles in uncovering the neural interactions during different cognitive states and brain diseases, especially the abnormal  $\theta$ - $\gamma$  PAC widely observed in epilepsy has provided several new insights into understanding the evolution of epilepsy. However, few studies pay attention to  $\beta$ - $\gamma$  PAC during epileptic phases. In the current study, we use MI method to calculate  $\beta$ - $\gamma$  PAC and construct  $\beta$ - $\gamma$  PAC-based functional brain networks, including phase-amplitude and amplitude-phase networks. We expect to seek a new perspective to understanding alterations of neural interactions during the epileptic evolution on the basis of  $\beta$ - $\gamma$  PAC, and to explore the alterations of  $\beta$ - $\gamma$  PAC-based functional brain networks during different epileptic phases. Statistical analysis shows that the PAC of epilepsy patients is abnormal, which is consistent with previous research results [16]. Specifically, there exists  $\beta$ - $\gamma$  PAC during epileptic phases, which changes significantly and differently for each EEG channel. Especially, the remarkably increased  $\beta$ - $\gamma$  PAC can be observed in most channels at the post-ictal period. Moreover, the between-channel MI values can be influenced by the information of phase and amplitude provided by different channels, which lead to statistical differences of several network properties between phase-amplitude

and amplitude-phase networks. Interestingly, both the phase-amplitude and amplitude-phase networks show that the averaged node degree and characteristic path length in the post-ictal period significantly different from that in the pre-ictal period. Besides, the average betweenness centrality in the post-ictal period significantly increases compared to that in the ictal period. These findings indicate that neural interactions within the brain change significantly along with the evolution of epilepsy, and  $\beta$ - $\gamma$  PAC may complement the current commonly utilized  $\theta$ - $\gamma$  PAC methods and provide a new perspective to view the dynamics of epilepsy.

The  $\beta$ - $\gamma$  PAC-based functional brain network may offer a new way to predict epileptic seizure. Statistically, the characteristic path length observed in the  $\beta$ - $\gamma$  PAC-based functional brain networks changes significantly during epileptic phases. Especially, both in the phase-amplitude and amplitude-phase networks, the characteristic path length in the ictal period is significantly reduced compared to that during the pre-ictal period. These observations indicate that the characteristic path length may contribute to the prediction of epileptic seizures. Actually, previous studies have also shown that the topological characteristics of brain functional networks can be applied to predict seizures. For example, an EEG-based functional brain network study has found that the characteristic path length increases continuously during the evolution of epilepsy, which can be used to predict seizures [34]. In another study, the functional brain network was jointly constructed with nine graph-theoretic parameters (assortativity coefficient, transitivity, clustering coefficient, strength of node, modularity, betweenness centrality, characteristic path length, global efficiency and radius), and had excellent epilepsy prediction performance [35]. Clearly, these studies further support our assumption that the characteristic path length may be a useful predictor for epileptic seizures, which is helpful for the early clinical diagnosis and treatment of epilepsy.

It has been demonstrated that the PAC and PAC-based functional brain networks greatly contribute to localizing epileptogenic zones. Specifically, a previous study based on the frontal EEG signals of epileptic patients found that the characteristics of EEG coupling strength in the interictal and pre-ictal periods can be used to accurately locate the epileptogenic regions, where the channels with strong PAC are mostly confined to the seizure onset zones and resection zones [36]. Similarly, the  $\theta$ - $\gamma$  PAC-based functional brain networks constructed by stereo-electroencephalography data acquired from patients with temporal lobe epilepsy indicated that there exists a strong cross-frequency coupling within epileptogenic regions during seizures, and the corresponding network is more regular than that in the interictal period, which suggests that PAC may contribute to identifying seizures and localizing epileptogenic zones [37]. Actually, the analysis of functional brain networks is also useful for accurately locating epileptogenic zones of patients with focal epilepsy. For example, Adkinson et al. used the centrality measurements to investigate characteristics of network nodes of patients with temporal lobe epilepsy and found that the electrode sites with maximum Katz centrality and degree centrality are closely related to epileptogenic zones

during seizures [38]. Goodale et al. used the resting state stereo-electroencephalography data acquired from patients with focal epilepsy to investigate the functional connectivity of sampled brain regions, and constructed a logistic regression model to predict epileptogenicity of individual regions, and found that the functional connectivities within the epileptogenic regions and between the epileptogenic regions and other structures are increased compared to that within nonepileptogenic structures [39]. Unlikely, we employed the MI method to construct the  $\beta$ - $\gamma$  PAC-based functional brain networks of pre-ictal, ictal and post-ictal periods, where statistical analysis shows that the changes of node degree of each channel are significant and different during the evolution of epilepsy. Particularly, both in the phase-amplitude and amplitude-phase networks, the node degree significantly increases in the post-ictal period compared to that in the pre-ictal period, which suggests that neural interactions during post-ictal period may be enhanced between some different brain regions. Of note, these alterations of node degree are very useful for identifying potential contributions of each channel to the evolution of epilepsy. Accordingly, both the node degree and betweenness centrality suggest that the F3-C3 channel may be an important node in epileptic phases in our work. Briefly, all these studies demonstrate that the PAC and PAC-based functional brain networks may provide a new way to locate epileptogenic zones.

The topological characteristics of  $\beta$ - $\gamma$  PAC-based functional brain networks may serve as a new point to understanding epilepsy. Indeed, numerous studies have shown that epilepsy is a network disease, which the related topological characteristics can provide new views to observe dynamical evolution of epilepsy [30], [40], [41], [42]. An EEG-based functional brain network study has found that the edge density slowly increases in the second half of the seizure and reaches a peak after the seizure, which suggests that the increased synchronization of neuronal activity may be an emergent self-regulatory mechanism underlying seizure termination [43]. Relative to the variations of network edges, the averaged node degree of the  $\beta$ - $\gamma$  PAC-based functional brain networks in our study also significantly changes during epileptic phases, which in the post-ictal period is significantly higher than that in the pre-ictal period. In addition, compared to the ictal period, the average betweenness centrality in the post-ictal period also significantly increased, which suggests that after the offset of seizures, the brain state may change from being dominated by multiple activated nodes to being dominated by fewer nodes. However, the characteristic path length in the ictal and post-ictal periods is significantly reduced compared to that in the pre-ictal period. Importantly, these observations can be supported by a previous study, which found that the characteristic path length corresponding to focal epilepsy slightly decreases with the onset of seizures and then slowly rebounds, while the characteristic path length corresponding to bilaterally spread focal epilepsy significantly decreases with the onset of seizures [44]. These findings suggest that the topological characteristics have a close association with the type of epilepsy, which can provide new insights into the evolution of epilepsy. Similarly, the statistical results of node degree, minimum spanning trees, and eccentricity

in current study indicate that neural interactions between F8-T8 and P3-O1 brain regions and other brain regions may be inhibited during seizures, which may also contribute to understanding the mechanism of epileptic seizures.

Of note, it has been demonstrated that PAC is not limited within a local brain region, which can also be observed between various functional brain regions [45]. As shown in our present study, alterations of between-channel MI values are significant during epileptic phases, which are different from that concentrating on PAC within local brain regions. More importantly, we found that there exists positive correlations between within-channel PAC and between-channel PAC, which also change along with the evolution of epilepsy. Due to that the phase and amplitude information of EEG signals are taken into account to calculate PAC, it is reasonable for us to speculate that compared to the within-channel PAC, the between-channel PAC may provide more evidence to show neural interactions during epileptic phases, as well as locating the seizure onset zone.

Despite that the  $\beta$ - $\gamma$  PAC is firstly employed in our study to examine the alterations of neural interactions during epileptic phases, we must admit that there are still some limitations in this work. For example, the EEG data analyzed in the work are acquired from the CHB-MIT public dataset, which has limited clinical information of each patient, lacks records of clinical symptoms or seizure frequency, and the labeling of seizure areas is not clear enough. Thus, it is difficult for us to accurately contrast the seizure onset zone with the locations identified by the  $\beta$ - $\gamma$  PAC. Notably, due to that the MI is least influenced by some confounding factors, such as noise data, short data epoch and low sampling rate, only MI-based PAC has been calculated in this work. Also, to avoid effects of spatial factor on MI values and reduce the computational cost, only eight channel signals have been selected to construct the  $\beta$ - $\gamma$  PAC-based functional brain networks. In addition, it should be noted that besides the  $\beta$ - $\gamma$  PAC calculated with MI method, various cross-frequency couplings have been proposed to investigate brain rhythms with different frequency bands [46], [47], [48]. In this study, despite that we particularly focused on the  $\beta$ - $\gamma$  PAC, couplings between other rhythms within the brain of epilepsy patients also deserve further investigation. Therefore, it is essential for us to systematically explore neural interactions with more cross-frequency couplings and more clinical EEG data with multi-channels, and explore the relationship between these neural interactions and patient clinical features in the future study.

## V. CONCLUSION

The  $\beta$ - $\gamma$  PAC-based functional brain networks have been constructed to investigate alterations of neural interactions during the evolution of epilepsy. Statistical analyses show that the between-channel  $\beta$ - $\gamma$  PAC significantly increases in the post-ictal period compared to that in the pre-ictal period. Similarly, the remarkably increased node degree and averaged node degree, as well as the decreased characteristic path length, can be observed in both phase-amplitude and amplitude-phase networks in the post-ictal period. In addition, the average betweenness centrality in the post-ictal period significantly increased compared to the

ictal period. More importantly, there exists positive correlations between within-channel MI values and between-channel MI values during epileptic phases. In conclusion, these findings suggest that the  $\beta$ - $\gamma$  PAC-based functional brain networks can provide a novel perspective to understanding the dynamical evolution of epilepsy, and may offer a new biomarker to locate the seizure onset zone.

## REFERENCES

- [1] J. Falco-Walter, "Epilepsy-definition, classification, pathophysiology, and epidemiology," *Seminars Neurol.*, vol. 40, no. 06, pp. 617–623, Dec. 2020.
- [2] E. Beghi, "The epidemiology of epilepsy," *Neuroepidemiology*, vol. 54, no. 2, pp. 185–191, Mar. 2020.
- [3] S. Sinha and K. A. Siddiqui, "Definition of intractable epilepsy," *Neurosciences*, vol. 16, no. 1, pp. 3–9, Jan. 2011.
- [4] W. O. Pickrell and P. E. Smith, "Treatment of resistant epilepsy," *Clin. Med.*, vol. 14, pp. s1–6, Dec. 2014.
- [5] N. Barot, "Networks in frontal lobe epilepsy," *Neurosurgery Clin. North Amer.*, vol. 31, no. 3, pp. 319–324, Jul. 2020.
- [6] G. Slinger, W. M. Otte, K. P. J. Braun, and E. van Diessen, "An updated systematic review and meta-analysis of brain network organization in focal epilepsy: Looking back and forth," *Neurosci. Biobehavioral Rev.*, vol. 132, pp. 211–223, Jan. 2022.
- [7] M. J. Vaessen et al., "White matter network abnormalities are associated with cognitive decline in chronic epilepsy," *Cereb. Cortex*, vol. 22, no. 9, pp. 2139–2147, Sep. 2012.
- [8] E. van Diessen, S. J. H. Diederend, K. P. J. Braun, F. E. Jansen, and C. J. Stam, "Functional and structural brain networks in epilepsy: What have we learned?," *Epilepsia*, vol. 54, no. 11, pp. 1855–1865, Nov. 2013.
- [9] A. Vetkas et al., "Identifying the neural network for neuromodulation in epilepsy through connectomics and graphs," *Brain Commun.*, vol. 4, no. 3, May 2022.
- [10] W. Stacey et al., "Emerging roles of network analysis for epilepsy," *Epilepsy Res.*, vol. 159, Jan. 2020, Art. no. 106255.
- [11] V. S. G. M. Tenorio, J. M. de Assis, and F. M. de Assis, "Functional and effective connectivity characterization of absence seizures," in *Proc. IEEE 27th Int. Conf. Syst., Signals Image Process.*, 2020, pp. 81–86.
- [12] J. M. den Heijer et al., "The relation between cortisol and functional connectivity in people with and without stress-sensitive epilepsy," *Epilepsia*, vol. 59, no. 1, pp. 179–189, Jan. 2018.
- [13] R. Rosch, T. Baldeweg, F. Moeller, and G. Baier, "Network dynamics in the healthy and epileptic developing brain," *Netw. Neurosci.*, vol. 2, no. 1, pp. 41–59, 2018.
- [14] O. Jensen and L. L. Colgin, "Cross-frequency coupling between neuronal oscillations," *Trends Cognit. Sci.*, vol. 11, no. 7, pp. 267–269, Jul. 2007.
- [15] S. Kullback and R. A. Leibler, "On information and sufficiency," *Ann. Math. Statist.*, vol. 22, no. 1, pp. 79–86, 1951. [Online]. Available: <http://www.jstor.org/stable/2236703>
- [16] Y. Salimpour, K. A. Mills, B. Y. Hwang, and W. S. Anderson, "Phase-targeted stimulation modulates phase-amplitude coupling in the motor cortex of the human brain," *Brain Stimulation*, vol. 15, no. 1, pp. 152–163, 2022.
- [17] D. C. Ghinda, Y. Salimpour, N. E. Crone, J. Kang, and W. S. Anderson, "Dynamical analysis of seizure in epileptic brain: A dynamic phase-amplitude coupling estimation approach," in *Proc. IEEE 43rd Annu. Int. Conf. Eng. Med. Biol. Soc.*, 2021, pp. 5970–5973.
- [18] H. Hashimoto et al., "Phase-amplitude coupling of ripple activities during seizure evolution with theta phase," *Clin. Neurophysiol.*, vol. 132, no. 6, pp. 1243–1253, Jun. 2021.
- [19] I. Mihaly, K. Orban-Kis, Z. Gall, A.-J. Berki, R.-B. Bod, and T. Szilagyi, "Amygdala low-frequency stimulation reduces pathological phase-amplitude coupling in the pilocarpine model of epilepsy," *Brain Sci.*, vol. 10, no. 11, Nov. 2020, Art. no. 856.
- [20] S. Rampp et al., "Dysmorphic neurons as cellular source for phase-amplitude coupling in focal cortical dysplasia type ii," *Clin. Neurophysiol.*, vol. 132, no. 3, pp. 782–792, 2021.
- [21] T. Murta et al., "Phase-amplitude coupling and the BOLD signal: A simultaneous intracranial eeg (ICEEG)-fMRI study in humans performing a finger-tapping task," *Neuroimage*, vol. 146, pp. 438–451, 2017.
- [22] M. Bočková et al., "Coupling between beta band and high frequency oscillations as a clinically useful biomarker for DBS," *npj Parkinson's Dis.*, vol. 10, no. 1, 2024, Art. no. 40.
- [23] M. Lundqvist, J. Rose, P. Herman, S. L. Brincat, T. J. Buschman, and E. K. Miller, "Gamma and beta bursts underlie working memory," *Neuron*, vol. 90, no. 1, pp. 152–164, 2016.
- [24] M. Chikermane et al., "Cortical beta oscillations map to shared brain networks modulated by dopamine," *bioRxiv*, 2024.
- [25] A. H. Shoeb, "Application of machine learning to epileptic seizure onset detection and treatment," Massachusetts Institute of Technology, 2009.
- [26] A. Delorme and S. Makeig, "EEGLAB: An open source toolbox for analysis of single-trial EEG dynamics including independent component analysis," *J. Neurosci. Methods*, vol. 134, no. 1, pp. 9–21, Mar. 2004.
- [27] W. O. Pickrell and P. E. Smith, "Treatment of resistant epilepsy," *Clin. Med.*, vol. 14, pp. s1–s6, Dec. 2014.
- [28] D. Liu, T. Cao, Q. Wang, M. Zhang, X. Jiang, and J. Sun, "Construction and analysis of functional brain network based on emotional electroencephalogram," *Med. Biol. Eng. Comput.*, vol. 61, no. 2, pp. 357–385, Feb. 2023.
- [29] S.-C. Hung et al., "Early recovery of interhemispheric functional connectivity after corpus callosotomy," *Epilepsia*, vol. 60, no. 6, pp. 1126–1136, Jun. 2019.
- [30] K. M. Park et al., "Progressive topological disorganization of brain network in focal epilepsy," *Acta Neurologica Scandinavica*, vol. 137, no. 4, pp. 425–431, Apr. 2018.
- [31] M. Rubinov and O. Sporns, "Complex network measures of brain connectivity: Uses and interpretations," *Neuroimage*, vol. 52, no. 3, pp. 1059–1069, 2010.
- [32] C. Stam, P. Tewarie, E. Van Dellen, E. Van Straaten, A. Hillebrand, and P. Van Mieghem, "The trees and the forest: Characterization of complex brain networks with minimum spanning trees," *Int. J. Psychophysiol.*, vol. 92, no. 3, pp. 129–138, 2014.
- [33] P. Hage and F. Harary, "Eccentricity and centrality in networks," *Social Netw.*, vol. 17, no. 1, pp. 57–63, 1995.
- [34] M. Christodoulakis, M. Anastasiadou, S. S. Papacostas, E. S. Papathanasiou, and G. D. Mitsis, "Investigation of network brain dynamics from eeg measurements in patients with epilepsy using graph-theoretic approaches," in *Proc. IEEE 12th Int. Conf. Bioinf. Bioeng.*, 2012, pp. 303–308.
- [35] A. A. H. Mubarak, "Predicting epileptic seizures from electroencephalography," Ph.D. dissertation, Univ. Southampton, Southampton, U.K., 2020.
- [36] H. Ma, Z. Wang, C. Li, J. Chen, and Y. Wang, "Phase-amplitude coupling and epileptogenic zone localization of frontal epilepsy based on intracranial EEG," *Front. Neurol.*, vol. 12, Sep. 2021, Art. no. 718683.
- [37] X. Liu, F. Han, R. Fu, Q. Wang, and G. Luan, "Epileptogenic zone location of temporal lobe epilepsy by cross-frequency coupling analysis," *Front. Neurol.*, vol. 12, Nov. 2021, Art. no. 764821.
- [38] J. A. Adkinson, R. Liu, I. Vlachos, and L. Iasemidis, "Connectivity analysis for epileptogenic focus localization," in *Proc. IEEE 32nd Southern Biomed. Eng. Conf.*, 2016, pp. 3–4.
- [39] S. E. Goodale et al., "Resting-state SEEG may help localize epileptogenic brain regions," *Neurosurgery*, vol. 86, no. 6, pp. 792–801, Jun. 2020.
- [40] S. Fang et al., "Decreasing shortest path length of the sensorimotor network induces frontal glioma-related epilepsy," *Front. Oncol.*, vol. 12, Feb. 2022, Art. no. 840871.
- [41] F. Xiao et al., "Functional brain connectome and sensorimotor networks in rolandic epilepsy," *Epilepsy Res.*, vol. 113, pp. 113–125, Jul. 2015.
- [42] T. Zhang et al., "Aberrant basal ganglia-thalamo-cortical network topology in juvenile absence epilepsy: A resting-state EEG-fMRI study," *Seizure-Euro. J. Epilepsy*, vol. 84, pp. 78–83, Jan. 2021.
- [43] K. A. Schindler, S. Bialonski, M.-T. Horstmann, C. E. Elger, and K. Lehnertz, "Evolving functional network properties and synchronizability during human epileptic seizures," *Chaos*, vol. 18, no. 3, Sep. 2008, Art. no. 033119.
- [44] N. Rungratsameetaweemana, C. Lainscsek, S. S. Cash, J. O. Garcia, T. J. Sejnowski, and K. Bansal, "Brain network dynamics codify heterogeneity in seizure evolution," *Brain Commun.*, vol. 4, no. 5, Sep. 2022, Art. no. fcac234.
- [45] A. C. E. Onslow, R. Bogacz, and M. W. Jones, "Quantifying phase-amplitude coupling in neuronal network oscillations," *Prog. Biophys. Mol. Biol.*, vol. 105, no. 1/2, pp. 49–57, Mar. 2011.
- [46] A. Shakeshaft et al., "Heterogeneity of resting-state EEG features in juvenile myoclonic epilepsy and controls," *Brain Commun.*, vol. 4, no. 4, Jul. 2022, Art. no. fcac180.
- [47] Y. Varatharajah et al., "Characterizing the electrophysiological abnormalities in visually reviewed normal EEGs of drug-resistant focal epilepsy patients," *Brain Commun.*, vol. 3, no. 2, 2021, Art. no. fcab102.
- [48] D. A. Hsu et al., "Correlation of EEG with neuropsychological status in children with epilepsy," *Clin. Neurophysiol.*, vol. 127, no. 2, pp. 1196–1205, Feb. 2016.